



Significant aerosol direct radiative effects during a pollution episode in northern China

J. Liu,^{1,2} X. Xia,² P. Wang,² Z. Li,^{1,3} Y. Zheng,¹ M. Cribb,³ and H. Chen²

Received 13 June 2007; revised 5 October 2007; accepted 7 November 2007; published 7 December 2007.

[1] Direct aerosol radiative effects during a heavy pollution episode that occurred in October 2004 over northern China are explored on the basis of ground-based and satellite-retrieved data. Aerosol loading rapidly built up due to a strong inversion and high relative humidity, with aerosol optical depth (AOD) at 550 nm increasing steadily from about 0.1 on October 1 to more than 1.0 six days later. Reflected irradiances at the top of the atmosphere (TOA) and surface irradiances change dramatically in response to the variation of the AOD. At the peak of the heavy pollution episode, the instantaneous reflected irradiances at the TOA increased by about 50 Wm^{-2} , while the instantaneous irradiances at the surface decreased by about 350 Wm^{-2} , resulting in solar heating of the atmosphere on the order of 300 Wm^{-2} . Solar radiation reflected to the space increased due to the build up of aerosols, indicating an overall cooling effect of the aerosols in the region. **Citation:** Liu, J., X. Xia, P. Wang, Z. Li, Y. Zheng, M. Cribb, and H. Chen (2007), Significant aerosol direct radiative effects during a pollution episode in northern China, *Geophys. Res. Lett.*, *34*, L23808, doi:10.1029/2007GL030953.

1. Introduction

[2] Due to the rapid growth of industrialization and urbanization in China, the mean aerosol optical depth (AOD) at 750 nm measured at 46 stations across China increased from 0.38 in 1960 to 0.47 in 1990 [Luo *et al.*, 2001]. The average AOD value in eastern China was about 0.55 in 2000 and escalated to 0.72 in 2005 [Zhao *et al.*, 2006]. Aerosols can modify the vertical profile of temperature in the atmosphere and the height of the boundary layer, and thus affecting local weather patterns and global climate [Ramanathan *et al.*, 2001]. Changes in some important meteorological variables over China during the past few decades have been associated with an increase in the aerosol loading and include a significant reduction in surface irradiance [Liang and Xia, 2005], resulting in cooling in eastern China [Li *et al.*, 1995] and a tendency toward increasing summer flooding in southern China and drought conditions in northern China [Xu, 2001; Menon *et al.*, 2002]. In order to better understanding the aerosol effects

on climate and the environment, researches on aerosol properties and its radiative effects have accelerated in China. Ground-based sunphotometer and lidar data, as well as satellite data, have revealed the spatial and temporal characteristics of aerosol optical properties over China [Li *et al.*, 2003; Xia *et al.*, 2005, 2006; Li *et al.*, 2007a; Papayannis *et al.*, 2007]. Some studies found that a thick layer of haze often covers northern China and that aerosol loading shows a large day-to-day variation [Li *et al.*, 2007b; Xia *et al.*, 2007a].

[3] In October 2004, a severe anthropogenic pollution event occurred over Beijing and its surrounding area. The visibility plummeted to about 200 m or less and the AOD at 550 nm was more than 1.0 over a vast portion of northern China during the peak pollution period (see below for details). The purpose of this paper is to discuss the aerosol effects on shortwave irradiance at the surface, at the top of the atmosphere (TOA) and within the atmosphere during this event. The aerosol effects at the surface are investigated using aerosol and radiation data collected at Xianghe, a baseline site near Beijing, which was established in 2004 under the auspices of the East Asian Study of Tropospheric Aerosols: An International Experiment (EAST-AIRE) [Li *et al.*, 2007a]. Instantaneous AOD retrievals from the Moderate Resolution Imaging Spectroradiometer (MODIS) and shortwave irradiance retrievals from the Clouds and Earth's Radiant Energy System (CERES) at the TOA are used to investigate the aerosol radiative effects at the TOA in northern China.

2. Data

[4] The Cimel sunphotometer, a multi-channel and automatic sun-and-sky scanning radiometer, was deployed at the Beijing (39.98°N , 116.38°E) and Xianghe (39.75°N , 116.96°E) sites. Measurements of direct and diffuse solar radiances are used to derive the AOD, the size distribution and the single scattering albedo (SSA) [Holben *et al.*, 1998]. Retrievals of the aerosol SSA can be achieved for AODs greater than 0.4 and for large solar zenith angles with an accuracy of ~ 0.03 [Dubovik *et al.*, 2000]. Two levels of the Aerosol Robotic Network (AERONET) product were used in this study: level 2.0 data (cloud-screened and quality-assured) and level 1.5 data (cloud-screened) when level 2.0 data were unavailable (downloaded from the AERONET website, <http://aeronet.gsfc.nasa.gov/>).

[5] The CERES sensor provides radiometric observations of the Earth-atmosphere system from three broadband channels: a shortwave channel ($0.3\text{--}5 \mu\text{m}$), a total channel ($0.3\text{--}200 \mu\text{m}$), and an infrared window channel ($8\text{--}12 \mu\text{m}$) [Wielicki *et al.*, 1996]. The appropriate angular distribution model is applied to convert the observed radiances to the

¹College of Environment Science and Engineering, Nanjing University of Information Science and Technology, Nanjing, China.

²Laboratory for Middle Atmosphere Global Environment Observation, Institute of Atmospheric Physics, Chinese Academy of Sciences, Beijing, China.

³Department of Atmospheric and Oceanic Science and Earth System Science Interdisciplinary Center, University of Maryland at College Park, College Park, Maryland, USA.

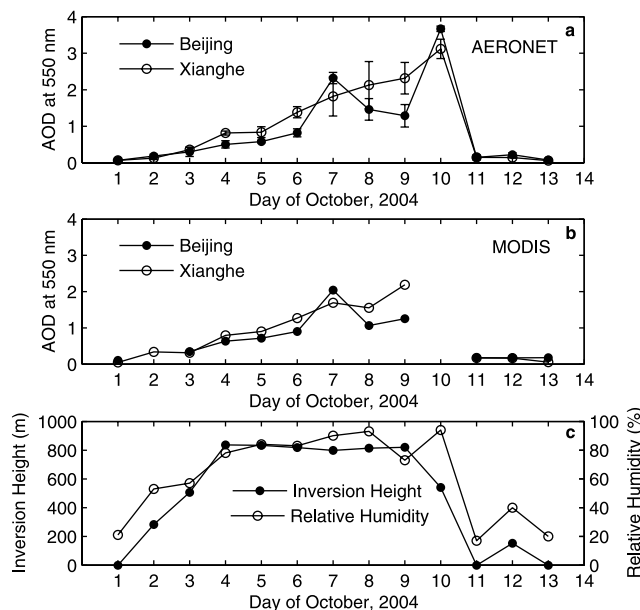


Figure 1. Time series of (a) daily mean AOD derived from AERONET and (b) instantaneous AOD retrieved from MODIS from October 1–13, 2004, at Xianghe and Beijing, and (c) the corresponding inversion height of the atmospheric boundary layer and near surface relative humidity measured by radiosonde at Beijing. Note that the vertical bars in Figure 1a represent the standard deviation of daily mean AOD.

irradiances or fluxes [Loeb *et al.*, 2005; Zhang *et al.*, 2005]. One set of products from the CERES instruments is the Single Scanner Footprint TOA/Surface and Clouds (SSF) collection of hourly products, which combines coarser resolution CERES measurements (about 20 km at nadir on the Terra platform) with scene information from the higher-resolution MODIS on the Terra platform. CERES/Terra SSF Edition 2B data were used in this analysis.

[6] Surface radiation data are collected at the Xianghe site (39.75°N, 116.96°E), located between two large cities (Beijing, 70 km to the northwest, and Tianjin, 70 km to the southeast). This is the first super-site of the EAST-AIRE [Li *et al.*, 2007a, 2007b]. Global surface shortwave radiations are obtained by summing the direct and diffuse components of radiation, which are separately measured by an Eppley normal incidence pyrliometer and a black-and-white radiometer, both mounted on an EKO STR-22 solar tracker. The field measurement uncertainties are estimated to be 3%, 6%, and 6% for direct, diffuse and global measurements, respectively [Stoffel, 2005]. The continuous high-quality measurements of aerosol, cloud and radiative quantities made at this site were used to examine aerosol radiative effects at the surface [Li *et al.*, 2007b; Xia *et al.*, 2007b].

3. Results

[7] Figure 1 presents the time series of AERONET and MODIS AOD values at 550 nm and the corresponding inversion height (IH) and near-surface relative humidity (RH) from October 1–13, 2004, over two sites: Beijing and Xianghe. The IH is defined as the height above ground

level at which air temperature increases with altitude, representing an “inversion” of the typical temperature decrease with height in the troposphere, and is derived from the temperature profile measured by radiosonde. Both daily mean AERONET (Figure 1a) and instantaneous MODIS AOD retrievals (Figure 1b) show the same pattern of variation over time. More insight was gained by Mi *et al.* [2007] into the comparison of satellite retrieved and ground-based AOD. The correlation coefficients of AOD between the AERONET and MODIS values both are 0.98 at two sites. The AOD values between October 7–9 exceed 1.0, which is significantly higher than values at other days in that month. The related IH and RH values during this period remained at about 800 m and above 80%, respectively (Figure 1c). This stable and low IH prevented aerosols from diffusing into higher levels of the atmosphere and the high RH fuelled aerosol hygroscopic growth, which enhanced the ability of aerosols to scatter shortwave radiation. This leads to high aerosol loading in the atmosphere, which is further supported by the Pennsylvania State University/National Center for Atmospheric Research mesoscale model data and MODIS/AOD data as well [Li *et al.*, 2005]. On October 11, the AOD dramatically dropped to about 0.2 due to the passage of a cold front across northern China.

[8] Ground-based aerosol and radiation data at Xianghe and satellite data from CERES/Terra are combined with a radiative transfer model to study the aerosol radiative effects at the surface, at the TOA and within the atmosphere. Aerosol properties retrieved from AERONET data, which include AOD, SSA and the asymmetry parameter at four wavelengths, are used as input to the Santa Barbara DISORT Atmospheric Radiative Transfer (SBDART) model [Ricchiazzi *et al.*, 1998]. Surface albedo is obtained from the MODIS43B product. The mean values of SSA and the asymmetry parameter at 440 nm during this pollution episode were about 0.86 and 0.70, respectively. The moderately low SSAs suggest a strong absorption by aerosols. The model is run with 33 altitude layers and four radiation streams. SBDART calculations agree with measurements to better than 3% [Halothore *et al.*, 2005]. To ensure temporal and spatial consistency, ground-based data were averaged within 30 minutes of the satellite overpass time, and the associated satellite data were averaged over a $40 \times 40 \text{ km}^2$ area centered on the Xianghe site.

[9] Figure 2 compares the observed and simulated instantaneous irradiances at the TOA (Figure 2a), at the surface (Figure 2b) and within the atmosphere (Figure 2c). The simulated irradiances agree with our measurements to within the measurement and simulation uncertainties. The correlation coefficients are generally larger than 0.99. The mean bias errors (MBE), i.e., the difference between mean simulation and mean measurement values, are 4.76 Wm^{-2} , -0.26 Wm^{-2} , and -6.30 Wm^{-2} at the TOA, at the surface, and within the atmosphere, respectively. The relatively larger discrepancies at the TOA are likely due to the larger uncertainties in the measurements. It is worth noting that a satellite scanning sensor does not measure TOA irradiances directly, but radiances. Conversion from radiances to irradiances entails the use of a set of the angular dependence models that are prone to large errors for instantaneous data [Li, 1996; Loeb *et al.*, 2005]. The radiative irradiances in the molecule atmosphere at the TOA, at the surface, and within

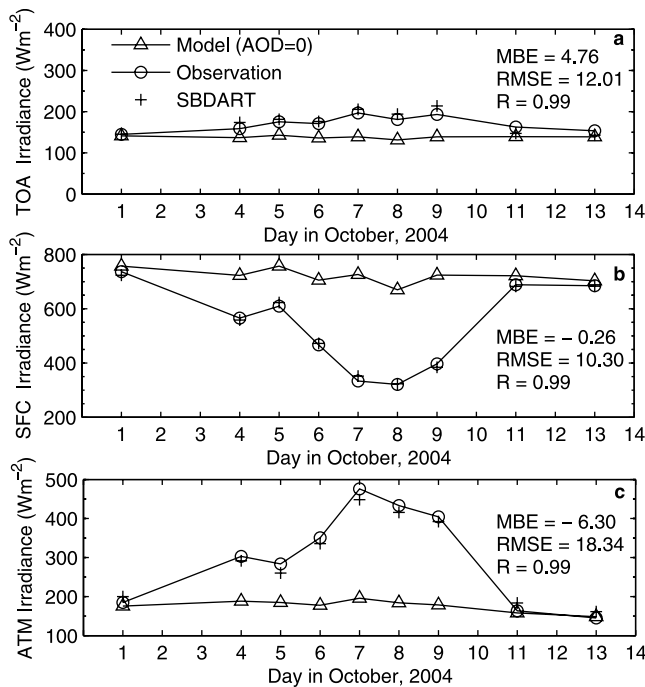


Figure 2. SBDART simulations without aerosols (triangles) and with aerosols (plus signs), and measurements of broadband solar irradiances (Wm^{-2}) (circles) from October 1–13, 2004, at Xianghe. Also included in the figure are the mean bias error (MBE: mean simulations minus mean measurements), root mean square error (RMSE), and correlation coefficients (R). (a) Reflected irradiance at the top of the atmosphere (TOA). (b) Downwelling irradiance at the surface (SFC). (c) Absorption within the atmosphere (ATM).

the atmosphere, are about 140 Wm^{-2} , 720 Wm^{-2} , and 180 Wm^{-2} , respectively. For the days with the large AOD values (October 7, 8 and 9), reflected irradiances at the TOA increased by about 50 Wm^{-2} , while the incoming surface irradiances decreased by around 350 Wm^{-2} , resulting in a solar heating of the atmosphere of about 300 Wm^{-2} . When the AOD at 550 nm changed from 0.1 to 2.8, the aerosol direct radiative forcing (ADRF) at the TOA changed from about -4 Wm^{-2} to -58 Wm^{-2} , and at the surface from about -20 Wm^{-2} to -390 Wm^{-2} .

[10] Note that the instantaneous effects of aerosols on surface irradiance depend heavily on the solar zenith angle. In order to isolate the dependence of surface irradiance on the AOD value, the diurnal mean aerosol forcing is computed to better represent the aerosol climatic effects. The ratio of the instantaneous solar irradiances measurements to the model simulations is computed, and then multiplied by the model diurnal cycle to convert the instantaneous measurements to corresponding diurnal cycle measurements. The derived curve is lastly integrated over 24 hours to obtain a diurnal mean solar irradiance. Figure 3 illustrates the diurnal mean ADRF as a function of AOD at 550 nm. The diurnal mean ADRF ranges from about -3 Wm^{-2} to -26 Wm^{-2} at the TOA, and from about -10 Wm^{-2} to -129 Wm^{-2} at the surface. The mean ADRF during this pollution event was -12 Wm^{-2} , -50 Wm^{-2} , and 38 Wm^{-2} at the TOA, the

surface, and within the atmosphere, respectively. These results imply a notable shortwave absorption of shortwave radiation within the atmosphere due to aerosols, which causes a strong warming in the atmosphere. This redistribution of shortwave irradiance induced by aerosols could alter atmospheric stability, thus influencing local wind circulation patterns and cloud dynamics and ultimately, affecting regional climate.

[11] Figure 4a shows the AOD at 550 nm obtained from MODIS and the reflected radiative fluxes at the TOA from CERES over northern China for October 8 (before the passage of the frontal system) and October 13 (after the passage of the frontal system). To eliminate the cloud effects, only those CERES pixels that were at least 99% cloud-free were used in the analysis. The results show that a vast portion of northern China was under clear-sky conditions on the two days. On October 8, a belt of pollution extended from the northeast to the southwest. Along this belt, the AOD increased from 0.8 to 1.4 and the TOA fluxes peaked at around $170\text{--}190 \text{ Wm}^{-2}$. On October 13, the AOD, in general, was less than 0.5 and TOA irradiances were less than 170 Wm^{-2} , indicating the end of the pollution event. To quantitatively understand the relationship between the AOD and TOA outgoing irradiances over northern China, the scatterplot of mean TOA upwelling shortwave irradiances as a function of mean AOD at 550 nm for different bins as a function of the associated mean TOA upwelling shortwave irradiances are shown in Figure 4b. Note that the spatial mean value of the broadband surface albedo obtained from CERES was about 0.16, with a standard deviation of 0.005, suggesting homogeneous surface characteristics during this pollution episode in northern China. The MODIS-retrieved AOD and the independently derived TOA upwelling irradiances from CERES show a high degree of correlation. The reflection of more solar radiation into space occurs during the build-up of aerosols

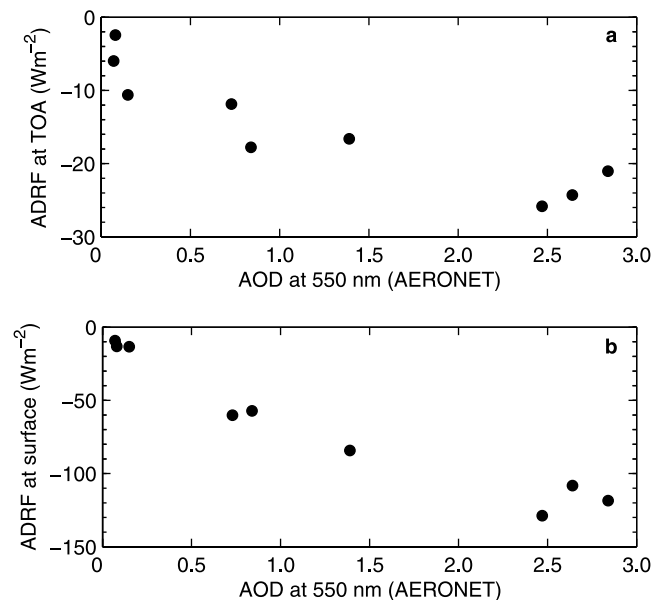


Figure 3. The observed daily aerosol direct radiative forcing (ADRF) as a function of AOD at 550 nm from October 1–13, 2004. (a) ADRF at the TOA from CERES. (b) ADRF at the surface from ground measurements.

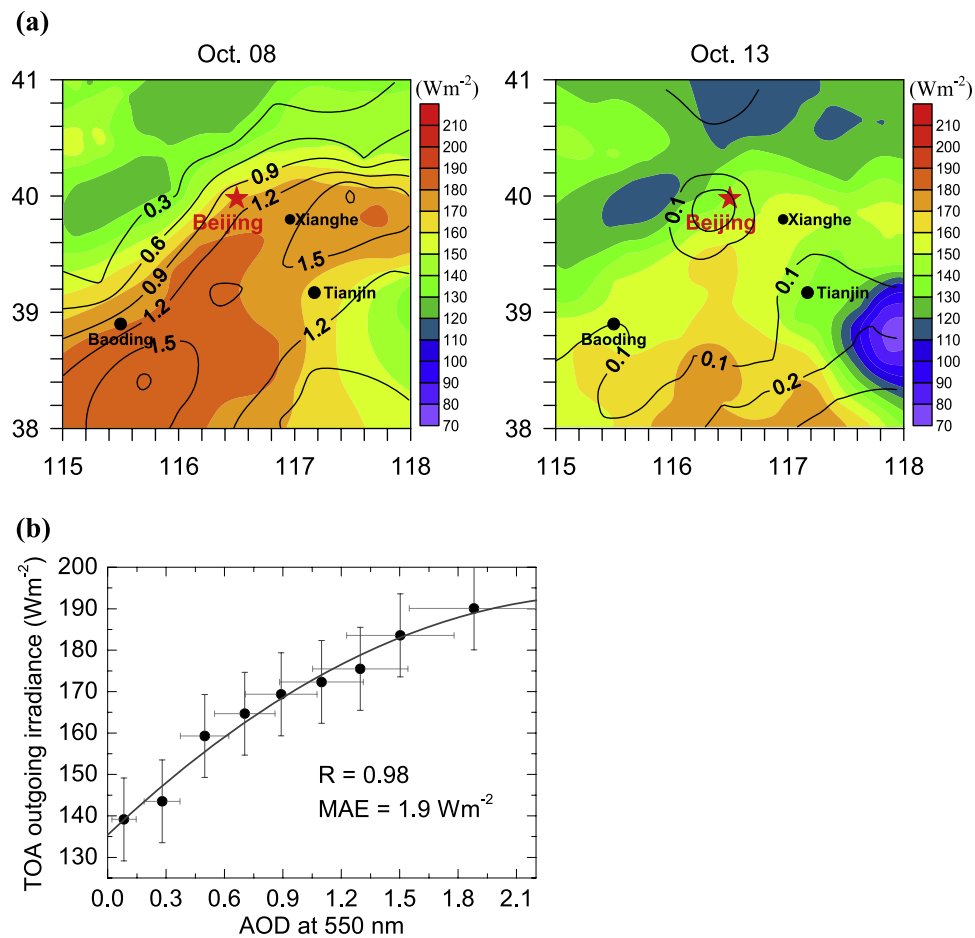


Figure 4. (a) AOD at 550 nm from MODIS and shortwave irradiance at the TOA from CERES for pristine and polluted days over northern China. Contours lines represent AOD and filled contours represent reflected irradiances (Wm^{-2}) at the TOA. The mean solar zenith angles on October 8 and 13 are 49.9° and 49.8° , respectively. (b) Scatterplot of the mean shortwave irradiances at the TOA from CERES as a function of the average MODIS-retrieved AOD at 550 nm for different bins over northern China. The vertical and horizontal bars represent the uncertainties of the TOA fluxes and AOD, respectively. A second-order polynomial fit is also shown by the solid line.

during the pollution event. A second-order polynomial fit is shown by the solid line which yields the following relationship: $F_{\text{TOA}} = -8.6\tau^2 + 44.6\tau + 135$, where τ represents AOD. The correlation coefficient is 0.98 and the mean absolute error (MAE) is 1.9 Wm^{-2} . This implies that the overall effect of aerosols is towards a cooling of the Earth's system.

4. Conclusions

[12] Using ground-based and satellite-retrieved aerosol and radiation data obtained during a heavy pollution episode that occurred in northern China, the dramatic variation of aerosol loading and consequent significant effects on the radiative energy budget were explored. The main conclusions are as follows.

[13] (1) Aerosol optical depth increased gradually from the background level to tens of times six days later and to more than 3.0 ten days later. This was chiefly due to persistent near-stagnant weather conditions over northern China during this time. The heavy aerosol loading finally

dropped dramatically to the background level as a cold front moved across northern China.

[14] (2) During the peak of the pollution episode, the instantaneous reflected irradiances at the TOA increased by about 50 Wm^{-2} , while the instantaneous irradiances at the surface dropped by about 350 Wm^{-2} , resulting in solar heating of the atmosphere on the order of 300 Wm^{-2} . The strong absorption within the atmosphere can enhance atmospheric stability and likely influence weather and climate.

[15] (3) There is a strong correlation between reflected fluxes at the TOA measured by the CERES instrument and MODIS-retrieved aerosol optical depths. A second-order polynomial equation was established which suggested that the overall effect of aerosols was to cool the Earth's system.

[16] **Acknowledgments.** The CERES data were obtained from the NASA Langley Research Center Atmospheric Sciences Data Center. The research is partly supported by the Knowledge Innovation Project of the Chinese Academy of Science (IAP07115), the National Science Foundation of China (40775009; 40250120071), the Urban Meteorological Research Foundation (UMRF200601), and the NASA Radiation Science Program (NNG04GE79G).

References

- Dubovik, O., A. Smirnov, B. N. Holben, M. D. King, Y. J. Kaufman, T. F. Eck, and I. Slutsker (2000), Accuracy assessments of aerosol optical properties retrieved from Aerosol Robotic Network (AERONET) Sun and sky radiance measurements, *J. Geophys. Res.*, *105*, 9791–9806.
- Halhore, R. N., et al. (2005), Intercomparison of shortwave radiative transfer codes and measurements, *J. Geophys. Res.*, *110*, D11206, doi:10.1029/2004JD005293.
- Holben, B. N., et al. (1998), AERONET—a federated instrument network and data archive for aerosol characterization, *Remote Sens. Environ.*, *66*, 1–16.
- Li, Z. (1996), On the angular correction of satellite-based radiation data: An evaluation of the performance of ERBE ADM in the Arctic, *Theor. Appl. Climatol.*, *54*, 235–248.
- Li, C. C., et al. (2003), Characteristics of distribution and seasonal variation of aerosol optical depth in eastern China with MODIS products, *Chin. Sci. Bull.*, *48*, 2488–2495.
- Li, C. C., J. T. Mao, Q. H. Liu, Z. B. Yuan, H. M. Wang, and Y. X. Liu (2005), Application of aerosol products from MODIS to atmospheric pollution in Beijing, *Sci. China Ser. D*, *35*, 177–186.
- Li, X. W., X. J. Zhou, and W. L. Li (1995), The cooling of Sichuan province in recent 40 years and its probable mechanism, *Qixiang Xuebao*, *9*, 57–68.
- Li, Z., et al. (2007a), Preface to special section on East Asian Studies of Tropospheric Aerosols: An International Regional Experiment (EAST-AIRE), *J. Geophys. Res.*, *112*, D22S00, doi:10.1029/2007JD008853.
- Li, Z., et al. (2007b), Aerosol optical properties and their radiative effects in northern China, *J. Geophys. Res.*, *112*, D22S01, doi:10.1029/2006JD007382.
- Liang, F., and X. A. Xia (2005), Long-term trends in solar radiation and the associated climatic factors over China for 1961–2000, *Ann. Geophys.*, *23*, 2425–2432.
- Loeb, N. G., S. Kato, K. Loukachine, and N. M. Smith (2005), Angular distribution models for top-of-atmosphere radiative irradiance estimation from the Clouds and the Earth's Radiant Energy System instrument on the Terra Satellite. Part I: Methodology, *J. Atmos. Oceanic Technol.*, *22*, 338–351.
- Luo, Y. F., D. R. Lu, X. J. Zhou, W. L. Li, and Q. He (2001), Characteristics of the spatial distribution and yearly variation of aerosol optical depth over China in last 30 years, *J. Geophys. Res.*, *106*, 14,501–14,513.
- Menon, S., et al. (2002), Climate effects of black carbon aerosols in China and India, *Science*, *297*, 2250–2253.
- Mi, W., Z. Li, X. Xia, B. Holben, R. Levy, F. Zhao, H. Chen, and M. Cribb (2007), Evaluation of the Moderate Resolution Imaging Spectroradiometer aerosol products at two Aerosol Robotic Network stations in China, *J. Geophys. Res.*, *112*, D22S08, doi:10.1029/2007JD008474.
- Papayannis, A., et al. (2007), Extraordinary dust event over Beijing, China, during April 2006: Lidar, Sun photometric, satellite observations and model validation, *Geophys. Res. Lett.*, *34*, L07806, doi:10.1029/2006GL029125.
- Ramanathan, V., P. J. Crutzen, J. T. Kiehl, and D. Rosenfeld (2001), Aerosols, climate, and the hydrological cycle, *Science*, *294*, 2119–2124.
- Ricchiazzi, P., S. Yang, C. Gautier, and D. Sowic (1998), SBDART: A research and teaching software tool for plane-parallel radiative transfer in the Earth's atmosphere, *Bull. Am. Meteorol. Soc.*, *79*, 2102–2114.
- Stoffel, T. (2005), Solar Infrared Radiation Station handbook, *ARM Tech. Rep. ARM-TR-035*, Natl. Renewable Energy Lab., Golden, Colo.
- Wielicki, B. A., B. R. Barkstrom, E. F. Harrison, R. B. Lee III, G. L. Smith, and J. E. Cooper (1996), Clouds and the Earth's Radiant Energy System (CERES): An Earth observing system experiment, *Bull. Am. Meteorol. Soc.*, *77*, 853–868.
- Xia, X. A., H. B. Chen, P. C. Wang, X. M. Zong, and P. Goloub (2005), Aerosol properties and their spatial and temporal variations over north China in spring 2001, *Tellus, Ser. B*, *57*, 28–39.
- Xia, X. A., H. B. Chen, P. C. Wang, W. X. Zhang, P. Goloub, B. Chatenet, T. F. Eck, and B. N. Holben (2006), Variation of column-integrated aerosol properties in a Chinese urban region, *J. Geophys. Res.*, *111*, D05204, doi:10.1029/2005JD006203.
- Xia, X., H. Chen, P. Goloub, W. Zhang, B. Chatenet, and P. Wang (2007a), A compilation of aerosol optical properties and calculation of direct radiative forcing over an urban region in northern China, *J. Geophys. Res.*, *112*, D12203, doi:10.1029/2006JD008119.
- Xia, X., Z. Li, P. Wang, H. Chen, and M. Cribb (2007b), Estimation of aerosol effects on surface irradiance based on measurements and radiative transfer model simulations in northern China, *J. Geophys. Res.*, *112*, D22S10, doi:10.1029/2006JD008337.
- Xu, Q. (2001), Abrupt change of the midsummer climate in central east China by the influence of atmospheric pollution, *Atmos. Environ.*, *35*, 5029–5040.
- Zhang, J., S. A. Christopher, L. A. Remer, and Y. J. Kaufman (2005), Shortwave aerosol radiative forcing over cloud-free oceans from Terra: I. Angular models for aerosols, *J. Geophys. Res.*, *110*, D10S23, doi:10.1029/2004JD005008.
- Zhao, C., X. Tie, and Y. Lin (2006), A possible positive feedback of reduction of precipitation and increase in aerosols over eastern central China, *Geophys. Res. Lett.*, *33*, L11814, doi:10.1029/2006GL025959.

H. Chen, J. Liu, P. Wang, and X. Xia, Laboratory for Middle Atmosphere Global Environment Observation, Institute of Atmospheric Physics, Chinese Academy of Sciences, Beijing 100029, China. (shunying0309@yahoo.com.cn)

M. Cribb, Department of Atmospheric and Oceanic Science and Earth System Science Interdisciplinary Centre, University of Maryland at College Park, 2207 CSS Building, College Park, MD 20742, USA.

Z. Li and Y. Zheng, College of Environment Science and Engineering, Nanjing University of Information Science and Technology, Nanjing 210044, China.